Inconsistency in 9 mm bullets: Correlation of jacket thickness to post-impact geometry measured with non-destructive X-ray computed tomography

John Thornby[a], Dirk Landheer[b], Tim Williams[b], Jane Barnes-Warden[c], Paul Fenne[c], Daniel Norman[a], Alex Attridge[a], Mark A. Williams[a]

[a] WMG, University of Warwick, CV4 7AL, United Kingdom

[b] Simpact Engineering Ltd, Unit 5, Benford Court, Lower Cape, Warwick CV34 5DA, United Kingdom

[c] Metropolitan Police Service, Operational Technology, 8-20 Loman Street, SE1 0EH, United Kingdom

Abstract

Fundamental to any ballistic armour standard is the reference projectile to be defeated. Typically, for certification purposes, a consistent and symmetrical bullet geometry is assumed, however variations in bullet jacket dimensions can have far reaching consequences. Traditionally, characteristics and internal dimensions have been analysed by physically sectioning bullets – an approach which is of restricted scope and which precludes subsequent ballistic assessment. The use of a non-destructive X-ray computed tomography (CT) method has been demonstrated and validated (Kumar et al., 2011 [15]); the authors now apply this technique to correlate bullet impact response with jacket thickness variations. A set of 20 bullets (9 mm DM11) were selected for comparison and an image-based analysis method was employed to map jacket thickness and determine the centre of gravity of each specimen. Both intra- and inter-bullet variations were investigated, with thickness variations of the order of 200 μm commonly found along the length of all bullets and angular variations of up to 50 μm in some. The bullets were subsequently impacted against a rigid flat plate under controlled conditions (observed on a high-speed video camera) and the resulting deformed projectiles were re-analysed. The results of the experiments demonstrate a marked difference in ballistic performance between bullets from different manufacturers and an asymmetric thinning of the jacket is observed in regions of pre-impact weakness. The conclusions are relevant for future soft armour standards and provide important quantitative data for numerical model correlation and development. The implications of the findings of the work on the reliability and repeatability of the industry standard V_{50} ballistic test are also discussed.

Keywords

- Ammunition variability;
- Armour standard;
- Ballistic impact;
- Bullet geometry;
- Jacket thickness;
- X-ray computed tomography

1. Introduction

Jacketed bullets typically contain a certain mass of heavy metal, such as lead, encased within a metal sleeve – the jacket. The jacket is intended to reduce friction within the rifle/gun barrel and ensures that the payload is uncompromised during delivery to the target. Depending on its velocity and the nature of the target a bullet's jacket might deform or rupture upon impact [1]. It has long been asserted that jacket thickness is a major contributor to bullet fragmentation and penetrative power [2]; however no major numerical modelling work to date has attempted to account for its impact on ballistic performance. Such models would be difficult to validate in the absence of a reliable method to measure jacket thickness variations non-destructively, both before and after impact. Present analytical models [3], [4], [5], [6], [7] and [8] consider only the gross geometry of bullets and make unjustified assumptions about the consistency and symmetry of the projectile and its casing. As such, a robust way to test correlation between ballistic performance and jacket thickness variation is desirable for the development of accurate numerical simulations.

Many methods of measuring the physical parameters of bullets have been documented. Destructive testing reveals detailed information regarding jacket thickness [9], however such methods are restrictive, may introduce inaccuracies due to deformation in the machining process and preclude studying geometric features of a bullet both pre- and post-impact. Although non-destructive radiographic techniques have been employed [10], [11], [12] and [13], they have not been exploited to their fullest potential. X-ray radiography lends itself to estimation of jacket thickness in a 2D plane; however, it cannot capture 3D geometry. X-ray computed tomography (CT) is a natural extension of X-ray radiography and possesses the capability to non-destructively analyse geometry in detail through the reconstruction of a three-dimensional volume.

This paper presents the application of X-ray CT [14] for the extraction of bullet geometry both before and after impact. Following the method prescribed by Kumar et al. [15] (summarised in Section 2), a set of 20, nominally identical, bullets were CT scanned prior to being subjected to ballistic performance tests under controlled conditions. The deformed projectiles were then re-scanned in order to observe and quantify the degree of deformation resulting from the impacts, with a view to correlating these ballistic performance indicators with geometric features of the un-deformed bullets prior to impact. This data will be used going forward to assist in the creation and validation of finite element models to more accurately describe ballistic impacts and help quantify the variability of threat level of ammunition of this kind.

2. CT scanning and image analysis

Computed tomography is a method of three-dimensional image reconstruction of an object from a number of 2D X-ray images (radiographs), taken at different angles. X-ray attenuation is dependent on the density and thickness of the object through which the beam has passed, so each projection image encodes information about the nature of the material in the volume. With sufficiently many projections, one may use numerical reconstruction algorithms [16] to disentangle this volume information and create a digital 3D representation of the volume. With appropriate X-ray conditions and post-processing methods, a volume element (voxel) resolution of below 10 μm is tenable.

2.1. CT scanning

A Nikon Metrology XTH 320 LC system was used for this study. This is an industrial micro-focus CT scanner with a 320 kV X-ray tube and a 2000 × 2000 pixel detector panel. Bullets were scanned using an appropriate electron acceleration voltage and a copper filter to exclude low energy X-rays, which prevents detector saturation and helps mitigate beam hardening effects which can cause artefacts in the reconstructed volume. A full discussion of this procedure and subsequent analysis is provided in [15] and [17]. All bullets were scanned prior to ballistic testing (Section 3) and then re-analysed using an identical method.

2.2. Bullet volume reconstruction and jacket segmentation

Three-dimensional volume data is reconstructed from radiograph images (Fig. 1a) using Nikon Metrology's proprietary software, *CT Pro*. Preferential attenuation of lower energy X-rays at shallow depth within the dense lead core results in beam hardening artefacts [18] which can be partially corrected for with software algorithms. A noise filtering algorithm is also available to enhance material voxels from the background.

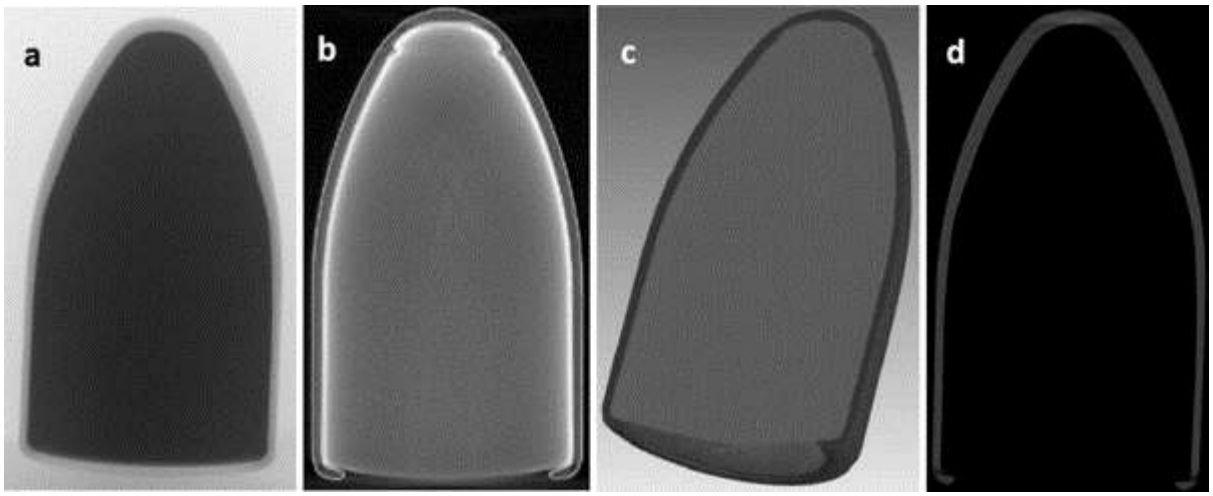

Fig. 1.

(a) A radiograph image of a bullet; (b) segmentation of a bullet jacket using a region growing algorithm and morphological operations; (c) 3D rendering of a complete bullet; (d) isolated jacket 2D slice.

The reconstructed volume is visualised in Volume Graphics' *VG Studio Max*. Volume data is first passed through a median filter which smoothes the images, facilitating the use of built-in algorithms to select Regions Of Interest (ROIs). ROIs are established for the "jacket" and the "core" of the bullet using a region growing tool which selects voxels with similar grey values that lie within a certain radius of a given seed point (Fig. 1b). The bright halo (caused by beam hardening within the lead core) provides a natural demarcation of the jacket and core. A 3D morphological closing operation is then performed on the ROI which fills in holes and discontinuities and also removes any sharp corners. Once segmented, the ROIs can be rendered (Fig. 1c) and 2D slices extracted in grayscale for further analysis (Fig. 1d).

2.3. Image analysis methodology

2.3.1. Extracting image slices

A cylinder is fitted to points selected randomly from the circumference of the jacket near the base of the bullet. This cylinder is used to verify the CT reconstruction scaling and as a geometrical reference, so that when the volume images are exported they are aligned consistently rather than to some arbitrary global coordinate frame. The cylinder axis therefore defines the orientation of the bullet and also a base plane, which can be taken as a reference for subsequent centre of gravity (COG) calculations. The jacket volume is then divided into slices one voxel thick perpendicular to the reference axis, resulting in a series of 2D greyscale cross-sectional images in which the bullet jacket material is evident as a grey ring against a black background. This image stack is exported for analysis and the procedure is repeated for the whole bullet (containing the lead core as well).

2.3.2. Establishing a physical reference

In this study, only bullet impacts without visible tumbling are considered. In order to compare jacket geometry variations before and after impact, a common coordinate system must be established. Three small notches and a double notch are physically carved on the underside of the bullet jacket at the cardinal points and are visible in the reconstructed CT image slices. Imaginary lines connecting diametrically opposite

notches define a reference axis system, and their intersection is taken as the central reference point about which all angular measurements are made (with the double notch taken as 0°). Since the notches are visible in both pre- and post-impact reconstructed images, one can reliably construct the same coordinate system for both cases and hence reproducibly establish the bullet orientation.

2.3.3. Calculation of jacket thickness

An analysis tool has been developed in-house, using *Matlab*, to calculate the jacket thickness [15] and [19]. The image slice stack is first loaded into computer memory and a cross sectional profile at 0° is computed from the 3D stack of images. This profile will have jagged edges due to inherent noise variations, so these are smoothed using morphological operations to flatten out small projected points and fill tiny undercuts on the profile image boundary. Binary images are obtained by thresholding and a parametric least squares Bezier curve fitting algorithm is employed to define the internal and external boundaries of the bullet profile image. The distance, normal to the outer boundary, is calculated analytically between these curves at sample points along the length of the bullet and corresponds to the jacket thickness. This procedure is repeated for profiles at other (discrete) angles until the whole surface of the bullet has been analysed. The reader is referred to [15] for a thorough discussion of the accuracy and validity of this method, including its verification against other physical assessment methods.

To visualise the jacket thickness, a 2D Cartesian colour map representation is adopted. Position coordinates on the map are the external length of the bullet jacket profile (from the tip) and the radial angle of that profile (relative to the bullet coordinate system); i.e. a pixel (x, y) on the map is a distance x from the tip of the bullet along the edge, at a radial angle y and is coloured according to the jacket thickness.

2.3.4. Calculation of centre of gravity

The COG is calculated using the relative weights of each voxel within the reconstructed volume, assuming densities of 11,340 kg/m^3 for lead and 7870 kg/m^3 for the steel jacket. A second set of image slices are read into computer memory, containing both the jacket and the lead core. Logical image operations are carried out to identify the pixels corresponding to jacket material and lead, which are then weighted accordingly to numerically ascertain the position of the COG; C_x, C_y and C_z, relative to the reference plane defined previously. It is then a trivial calculation to derive the position of the COG relative to the tip of the bullet.

3. Ballistic testing

Typically, DM11 bullets fired from a hand gun can be stopped with a soft armour system. In such events, however, the jacket may rupture, depending on the velocity of the bullet and the performance of the armour. It is hypothesised that the threat level of a bullet is influenced by the jacket thickness and this could affect the performance of an armour system; however it is difficult to decouple the simultaneous variability of both the projectile and the target armour.

The motivation for this study is to investigate bullet deformations similar to those seen in impacts with soft armour. The ballistic test was designed to replicate as closely as possible the characteristic mushroom-like bullet deformation, shown in Fig. 2, typical of an impact with soft armour. But, in order to eliminate any variation in target performance, a flat, hardened steel plate target was chosen instead of a soft armour system. Due to the difference in the exchange of energy and momentum between projectile and target in this kind of impact, it was necessary to use test velocities significantly lower than the normal operational velocity of a DM11 bullet in order to avoid fragmentation. Pilot tests revealed empirically that an impact velocity in the region of 120 m/s led to bullet deformations in the regime where the jacket begins to rupture. For a variety of bullets, the typical velocities for fragmentation to occur on impact with unyielding targets are given in [20].

Fig. 2.

Characteristic “mushroom” deformation of a DM11 bullet after impact with soft armour.

20 DM11 bullet heads from two different manufacturers were tested at Hallrite Precision Engineering ballistic range in Chesterfield, Derbyshire (UK). In total 15 ‘Rheinisch-Westfälischen Sprengstoff-Fabriken’ (RWS) and 5 ‘Gold Medal’ (GM) bullet heads were tested. The objective of the tests was to generate pairs of bullets, deformed by ballistic collision under identical conditions, to be compared in detail with the Micro CT scanner at WMG for subsequent use in ballistic impact modelling at Simpact Engineering Ltd.

A standard configuration was used to fire the bullets via a remotely operated breach. Fig. 3(left) shows the experimental setup including the painted steel plate; a High Speed Video (HSV) camera and 3 lighting units. The HSV had a close to square-on view of the target, facilitating imaging the bullets perpendicular to their direction of motion, shown in Fig. 3(right). The level of light generated allowed for a good depth of field and an appropriate frame rate of 28,000 fps. A small magnetic rule was attached to the strike face adjacent to the impact zone for reference. The HSV output was used to verify the absence of bullet yaw. Bullets were selected for analysis for which there was no detectible yaw within the resolution of the HSV system; i.e. any yaw was less than one degree.

Fig. 3.

Experimental setup (left): The ballistic target is a flat, hardened steel plate. Three lighting units provide necessary illumination for a High Speed Video (HSV) camera which captures the impact (right).

Bullet velocity measurement was provided by the range chronograph and verified with the High Speed Video. In order to attain the target velocity of 120 m/s, a relatively small amount of propellant charge (~2.5 grains) was required. In this regime, however, low pressures within the bullet casing and friction effects in the breach become predominant, resulting in a challenge to produce consistent impact velocities. At normal operational velocities these effects are much less pronounced and do not cause complications. To mitigate the problem, a foam ‘filler’ material

was placed above the powder in each shot to give a consistent powder distribution and encourage even combustion. Nevertheless, a significant spread of bullet velocities was observed and on one occasion a misfire occurred. Bullet impact velocities are tabulated in Table 1 and Fig. 3 illustrates the post-impact bullet heads. Bullets 11–15 (red box) are the GM specification and the rest are RWS. It can be seen that the GM spec provided more consistent bullet velocities and deformation in this low velocity regime.

Table 1.

Manufacturer and velocity information for each bullet in the study (bullets 1–10 were test shots).

Bullet #	Manufacturer	Velocity (m/s)	Bullet #	Manufacturer	Velocity (m/s)
11	GM	116.8	21	RWS	Misfire
12	GM	112.0	22	RWS	147.9
13	GM	114.0	23	RWS	153.8
14	GM	116.3	24	RWS	127.0
15	GM	120.8	25	RWS	139.9
16	RWS	134.8	26	RWS	153.8
17	RWS	123.2	27	RWS	145.3
18	RWS	146.1	28	RWS	143.4
19	RWS	130.2	29	RWS	156.4
20	RWS	150.8	30	RWS	102.8

4. Observations and analysis

The bullets were retrieved and identified for close inspection and CT scanning at WMG. For comparative assessment, bullets 11, 14 and 15 were chosen from the GM specification because they had very similar impact velocities. Their consistent ballistic performance may be ascribed to their physical dimensions, which seem to be more compatible with the shell casings used in the ballistic test series. All five GM bullets had a measured diameter of 9.00 mm, implying a tighter fit within the case than the RWS bullets, which measured 8.98 mm. It is speculated that this goodness of fit leads to more consistent pressure within the casing. Furthermore, a black powder residue was found on some of the RWS casings, indicating incomplete combustion.

Fig. 5 shows the three deformed GM bullet heads side by side. It can be seen that they exhibit very similar overall deformation. The flat face of each impacted bullet head shows a concentric ring of lighter colour. This is believed to be the thicker ring of jacket material described in Section 4.1. Bullets 16 and 17 were also chosen from the RWS bullet samples, due to the similarity of their deformation.

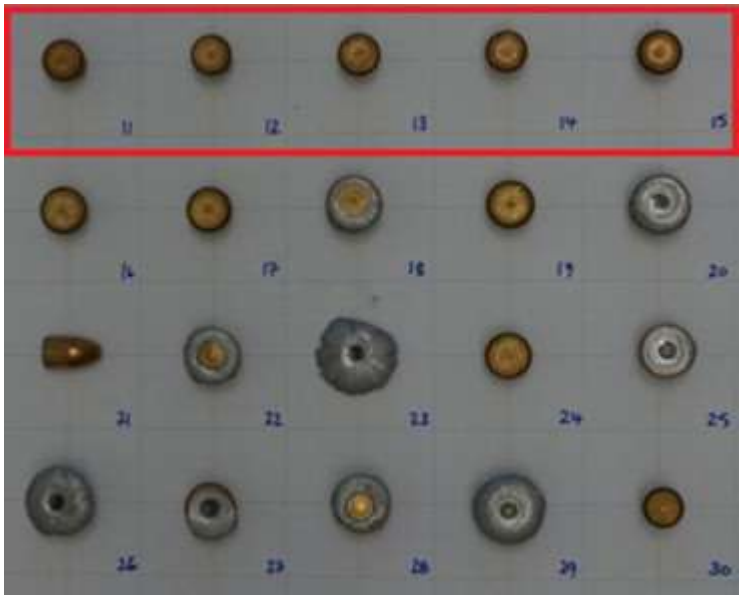

Fig. 4.

Bullets 11–30 (post-impact), demonstrating the degree of variation in deformation. The top row (red box) are GM specification and the rest are RWS. (For interpretation of the references to colour in this figure legend, the reader is referred to the web version of this article.)

Fig. 5.

Post-impact bullet heads 11 (116.8 m/s), 14 (116.3 m/s) and 15 (120.8 m/s), GM specification.

4.1. Pre-impact comparison

Fig. 6 shows the jacket thickness colour plot for bullet 11, prior to ballistic impact. For clarity, the Cartesian plot (described in Section 2.3.3) is shown alongside a polar representation. This data is representative of the other bullets in the sample and overall jacket thickness variations have a similar distribution to those reported by Kumar et al. [15] – although with a greater variation towards the tip of the bullet. The same interesting 'ring' feature near the tip is present in all of the GM bullets, visualised as a red band in the thickness plot. The red band equates to 525 μm jacket thickness locally, compared to approximately 400 μm at the tip and shoulder.

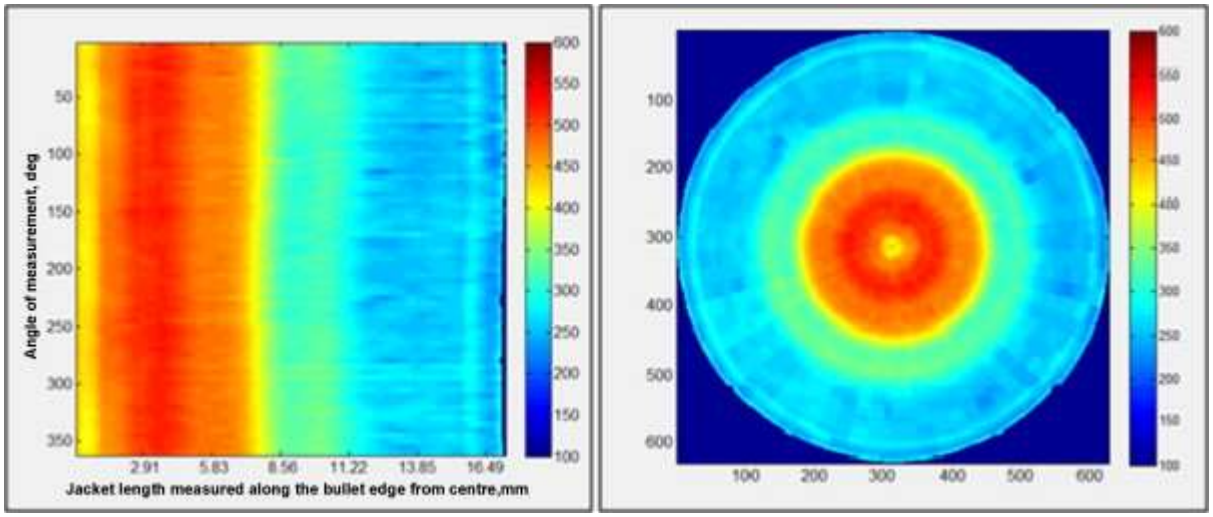

Fig. 6.

Pre-impact jacket thickness colour plots for bullet 11: Cartesian representation (left) and polar representation (right). All jacket thicknesses are measured in μm.

In bullets 14 and 15, the ring pattern is noticeably thicker by around 100 μm; the tip of bullet 11 is thinner by around 100 μm and the rear section of bullet 11 is thinner by around 70 μm, shown in Fig. 7 (Cartesian plots for bullets 14 and 15 can be found in Fig. 12 and Fig. 13). A comparison of intra-bullet jacket thickness for bullets 11, 14 and 15 is shown in Table 2. It can be seen that there is an angular variation in jacket thickness of order 50 μm at equivalent positions along a bullet's length.

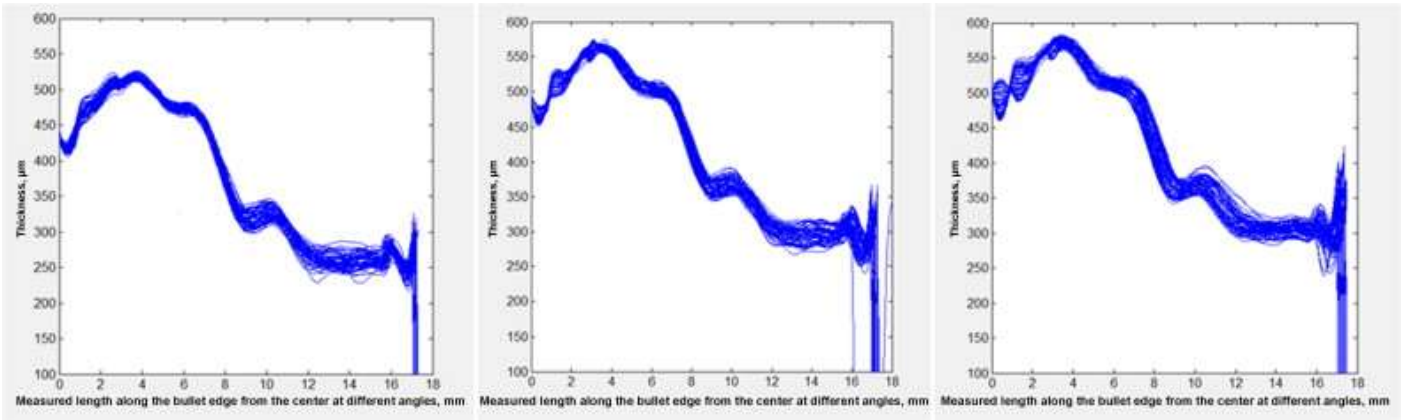

Fig. 7.

Jacket thickness variation (μm) for bullets 11 (left), 14 (centre) and 15 (right), pre-impact. Lines represent the thickness profiles at different radial angles around the bullet. A spread of as much as 50 μm is observed at equivalent positions along the bullets' length.

Table 2.

Mean intra-bullet jacket thickness angular variation (μm), pre-impact.

Length position	**0 mm**	**2 mm**	**4 mm**	**6 mm**	**8 mm**	**10 mm**	**12 mm**	**14 mm**
Mean jacket thickness angular variation (μm)	16.7	43.1	32.0	36.1	51.4	44.4	52.8	54.2

4.2. Post-impact comparison

The following sequence of events has been identified in the deformation of the bullet:

1. The bullet tip contacts the target. The contact generates normal stress, locally thinning the jacket. See schematic representation in Fig. 8.

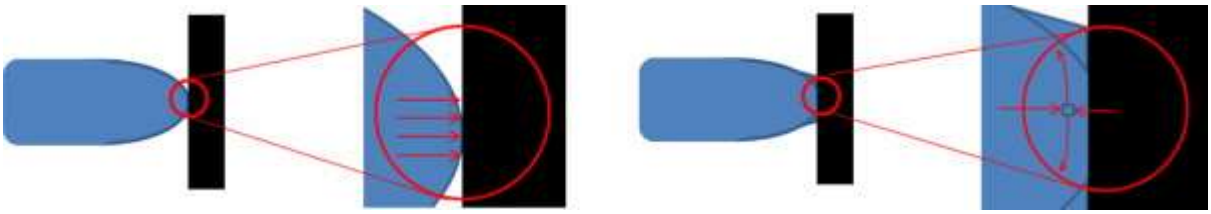

Fig. 8.

Stage 1 (left): contact generates normal stress, locally thinning the jacket. Stage 2 (right): compressive stress and tangent tensile stress results in flattening of the tip.

2. A combination of radial compressive stress and tangent tensile stress results in flattening of the tip. See schematic representation in Fig. 8.

3. An internal pressure wave starting at the tip from the relatively soft lead core causes tangent tensile stress in the jacket, stretching the diameter. Where the jacket is in contact with the target, friction counteracts this stretching, see illustration in Fig. 9. The edge of the contact zone, not the area of largest diameter change, is where ultimately rupture of the jacket will occur if the impact velocity is high enough. This is supported by Fig. 4. In case of impact with a soft target such as soft armour, rupture is most likely to occur in the zone that undergoes the largest diameter change. The kinematics of bullet deformation on impact with an unyielding target is described in detail in [21].

of bullet deformation on impact with an unyielding target is described in detail in [21].

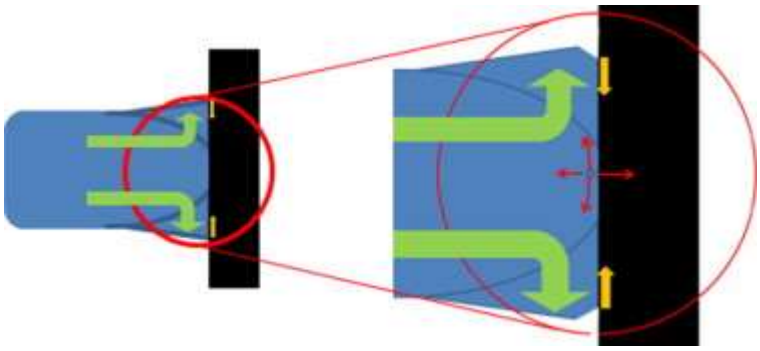

Fig. 9.

Stage 3: Internal pressure wave causes tangent tensile stress in the jacket, stretching the diameter. Where the jacket is in contact with the target, friction counteracts this stretching.

In the case of impact with a soft target, such as soft armour, rupture is most likely to occur in the zone that undergoes the largest diameter change. Typically, the latter is initiated by the rifle marks on the jacket, demonstrated in Fig. 2 which shows a typical DM11 stopped on soft armour. In such experiments macroscopic elongations exceeding 100% are observed. This is only possible as a result of the multi axial stress condition [22]. In the case of the flat hardened steel target, rupture occurs on the edge of the contact zone before macroscopic elongations of this magnitude can occur in the unsupported part of the jacket – evidenced by the data in Table 3 which summarises the various physical properties of the five bullets under consideration. This does not make this jacket thickness variation study less relevant.

Table 3.

Physical properties of the bullets pre- and post-impact. Length is measured (with a screw gauge micrometre) from the tip of the bullet to the base of the lead core. C_z is the distance of the *z*-component of the COG from the bullet tip, calculated from the CT scan voxel weightings. Hardness is the average of ten 500 g_F micro-Vickers hardness tests. Elongation is the percentage increase in the post-impact diameter at the widest point, measured from the CT scan data.

Bullet	**Pre-impact**			**Post-impact**			**ΔCOG, C_z (mm)**	**Elongation**	**μ-Vickers test**		
	Mass (g)	**Length (mm)**	**COG, C_z (mm)**	**Mass (g)**	**Length (mm)**	**COG, C_z (mm)**		**Max diameter increase (%)**	**Mean jacket hardness (HV500 g_F)**	**Std Dev**	**Std error**
11	8.0088	15.80	8.99	8.0083	10.49	3.63	5.36	29.9	180.3	10.3	3.3
14	8.0251	15.80	9.05	8.0244	10.50	3.90	5.15	27.1	177.2	15.4	4.9
15	8.0203	15.91	9.13	8.0196	10.19	3.30	5.83	33.3	176.4	16.0	5.1
16	8.0114	15.84	9.23	8.0105	8.51	1.70	7.53	43.6	177.8	16.1	5.1
17	7.9992	15.62	8.73	7.9978	9.12	2.07	6.66	37.8	172.3	12.8	4.0

The change in distance of the centre of gravity (COG) to the tip of the projectile is a measure of the mechanical compliance. A larger compliance typically relates to a reduction in penetrative power. Table 3 also demonstrates the COG shift for the 3 GM and the 2 RWS bullets. For bullet 11 the COG position moves forward by 5.36 mm whereas in bullet 14 it moves forward by 5.15 mm. This increase of 0.21 mm in forward deformation is thought to be due to the lower jacket thickness observed in bullet 11 (given their comparable mass and impact velocity). For bullet 15, the COG position moved by a further 0.26 mm and this is considered to be most likely due to the higher impact velocity (+7% kinetic energy).

By nature, the pressure load in a cylinder can cause unstable behaviour, dependent on the material hardening properties of the jacket. Based on micro-Vickers hardness measurements, shown in Table 3, the hardening properties of all bullets are found to be consistent within standard error. Any irregularities in wall thickness along the circumference of the jacket can trigger instability, ultimately resulting in rupture. Fig. 10 shows an example of a cross section of the CT data for a deformed bullet (left) and a slice of bullet 14 at the point at which the jacket thickness has thinned the most (90°).

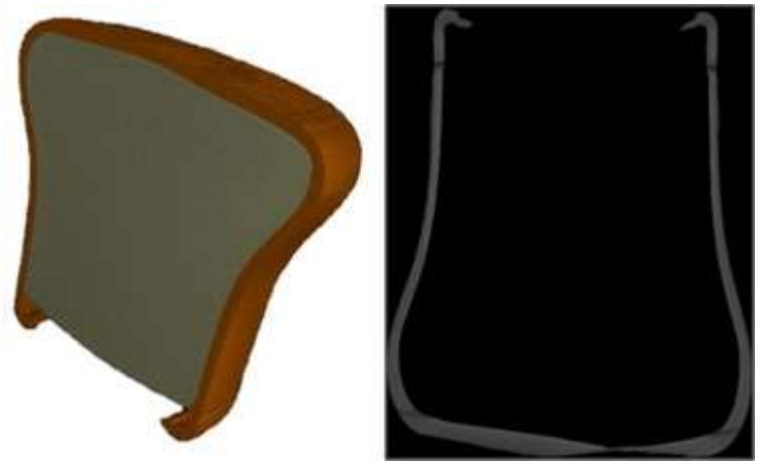

Fig. 10.

3D view of a section through the CT data of a deformed bullet and cross section of bullet 14.

Fig. 11, Fig. 12 and Fig. 13 show the un-deformed and deformed Cartesian plots for the GM bullet heads 11, 14 and 15 respectively. All three of the deformed plots show distinct areas of thinning and it is believed that these areas would be the first to rupture if the bullet continued to deform. There is a possible link between the angular position of jacket thinning in the deformed bullets and the pre-impact jacket thickness distribution – although this could be coincidental and further research is required to investigate the nature of this correlation. In bullets 14 and 15 the 'ring' is disrupted in thickness in this area. This leads to a local increase in hoop stress which may have led to the pronounced jacket thinning in the deformed bullet.

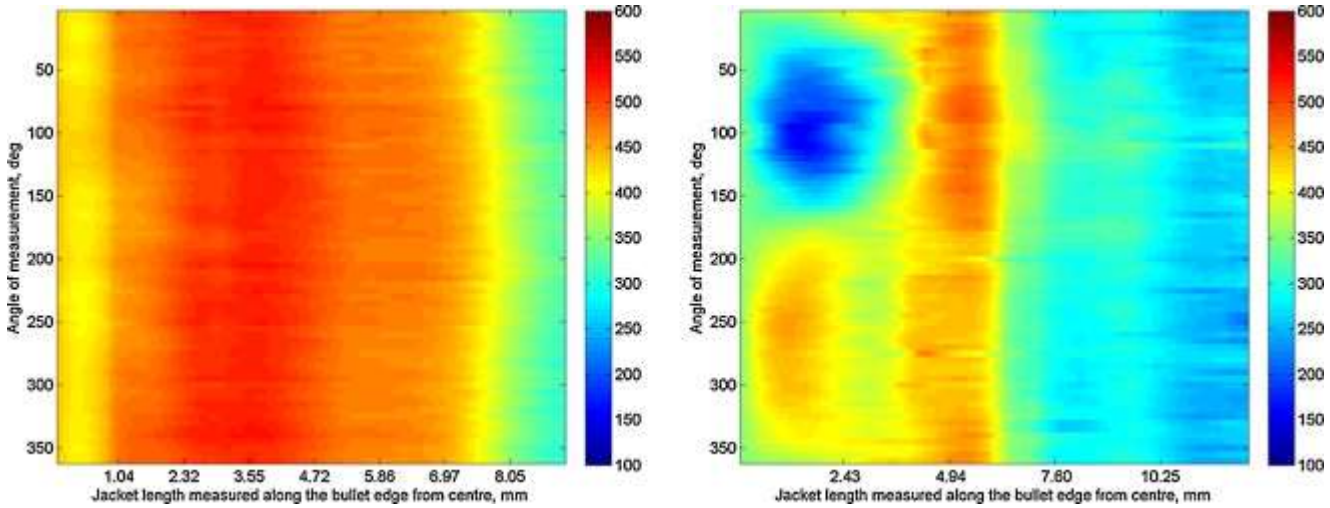

Fig. 11.

Cartesian thickness plot in µm for Bullet 11, pre-impact (left), post-impact (right).

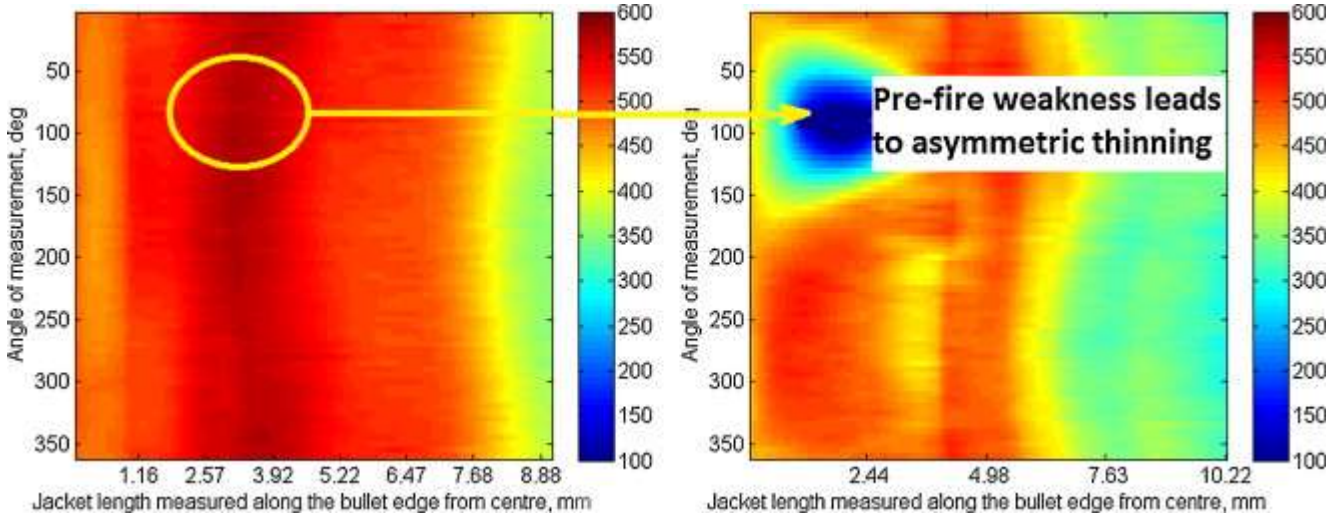

Fig. 12.

Cartesian thickness plot in µm for Bullet 14, pre-impact (left), post-impact (right).

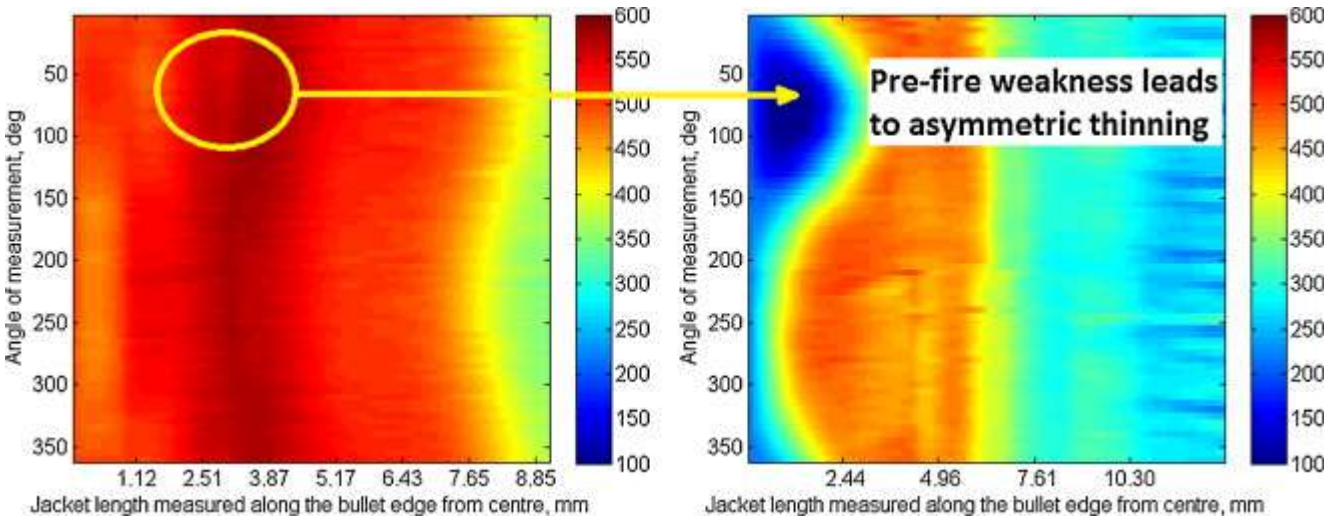

Fig. 13.

Cartesian thickness plot in µm for Bullet 15, pre-impact (left), post-impact (right).

Fig. 14 and Fig. 15 show the Cartesian and polar jacket thickness plot for the RWS bullet heads 16 and 17.

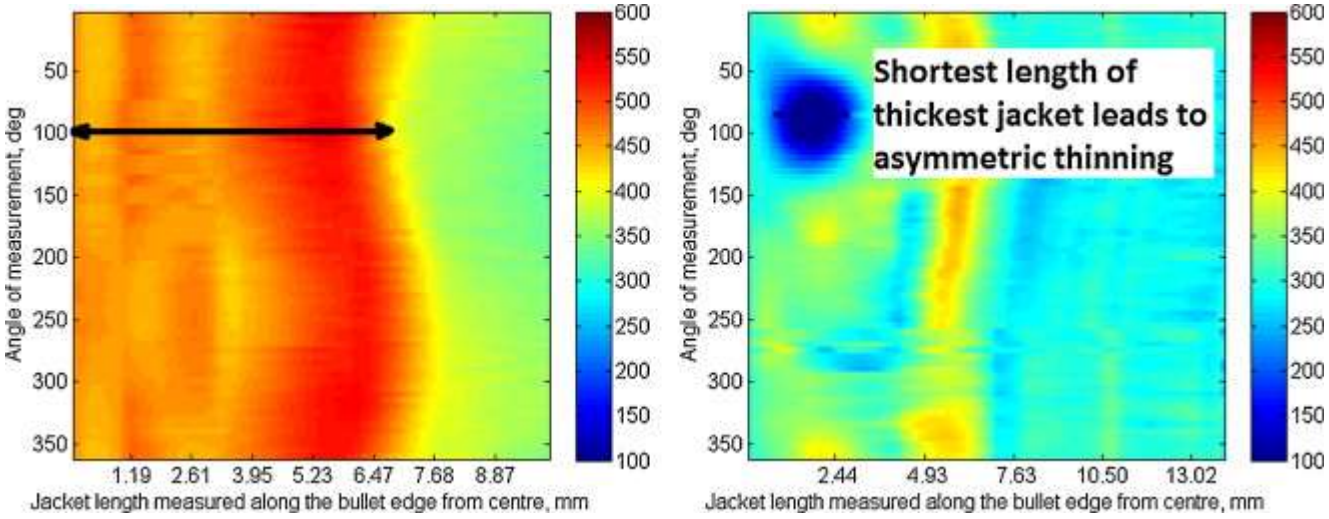

Fig. 14.

Cartesian thickness plot in µm for Bullet 16, pre-impact (left), post-impact (right).

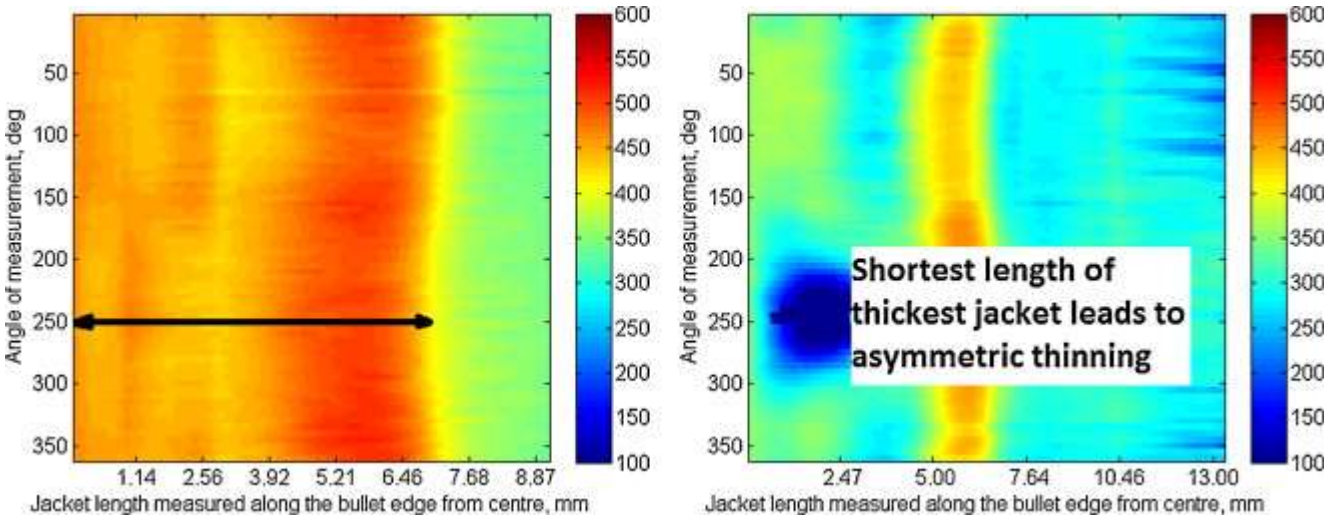

Fig. 15.

Cartesian thickness plot in µm for Bullet 17, pre-impact (left), post-impact (right).

The RWS bullet heads did not exhibit the distinct ‘ring’ seen in the GM bullet heads, but the deformation plots again show distinct areas of thinning. There is evidence to suggest that the angular position at which post-impact jacket thinning is maximal corresponds to the angular position at which the distance to the shoulder was shortest in the un-deformed bullet. This implies that rupture occurs asymmetrically on the bullet face as a result of asymmetry in the original geometry of the jacket.

5. Conclusions

This study applies the non-destructive X-ray computed tomography (CT) method developed by Kumar et al. to bullets that have been impact tested. A set of 20 bullets (9 mm DM11) were measured and pre-impact thickness variations of the order of 200 μm along the length were found commonly across all bullets and angular variations of up to 50 μm were found in several.

The study highlights the difficulty in achieving consistent bullet velocities at target speeds lower than the operational norm. Of the two different DM11 bullet specifications tested, the GM bullet heads provided the most consistent bullet velocities. This is most likely because, at low test velocities, the geometric fit within the casings is more critical than at operational velocities. The firing system utilised for this test series was not designed to achieve such low target velocities and a compressed air system would be more appropriate for further work, but nevertheless this study highlights a difference in performance of nominally identical bullets under similar conditions.

A measure of the bullet mechanical compliance is the movement of the calculated COG on impact. The study of the small batch of valid results (i.e. similar velocities) suggests that larger bullet deformations may occur in regions of pre-impact jacket weakness – where the thickness is least or supporting material is radially asymmetric. Thinning that can lead to rupture appears to be influenced by jacket thickness variations. For impact on a flat, rigid target the most likely area for rupture of the jacket is affected by the radial forces transferred between the bullet tip and target. Jackets stopped on soft armour tend to rupture at the area of largest diameter change. In both cases, local thinner areas in the jacket are stressed higher for the given loads (pressure in the core and friction with the target). Dependent on the material hardening properties [23] this results in instability, ultimately leading to rupture. This suggests that manufacturing tolerances and inter-manufacturer variability may be significant contributing factors to a bullet's threat level, and that jacket thickness may be a more important performance indicator than was first thought.

It is believed that the basis of the observed trends is more than just kinematics, presented in [21], but further testing is required in order to verify this assertion. For a more detailed and conclusive analysis it would be desirable repeat this study on a larger, more statistically significant sample. Going forward, the authors intend to test their hypothesis by way of a blinded experiment, in which deformations will be predicted semi-quantitatively from pre-impact data as opposed to searching for post hoc correlations.

The results from this study can be used to refine and correlate finite element models of the DM11 bullet to include jacket thickness variation. The refined bullet model can subsequently be used to assess the sensitivity of soft armour performance to variations in bullet jacket thickness. Note that at that stage rifle marks will have to be considered.

This method of analysis can be used to support the development of standards related to bullet characterisation in the personal protection industry. Going forward, the authors aim to apply the method to a range of threats and use the results of this study to validate finite element modelling of ballistic impacts that feed into simulations of events such as the V_{50} soft armour test [24]. If inter-manufacturer variability is found to be as significant as is believed, then it could serve to call for more stringent quality control in the ammunition used for such tests in the future.

Acknowledgements

The authors would like to thank Jagadeesha Kumar, Karol Tomczyk and Ian McDonnell for their contributions to the CT image processing and analysis framework, and to Peter Hall at Hallrite Precision Engineering for his assistance with ballistic tests. This work was carried out as part of the PVCIT Centre of Excellence Research Centre, part funded by Advantage West Midlands and the European Regional Development Fund.

References

[1] P.J.T. Knudsen, P. Theilade; Terminal ballistics of the 7.62 mm NATO bullet autopsy findings, Int. J. Legal Med., 106 (2) (1993), pp. 61–67

[2] P.J.T. Knudsen, J.S. Vigsanæs, R. Rosmussen, P.S. Nissen; Terminal ballistics of the 7.62 mm NATO bullets: experiments in ordnance gelatine, Int. J. Legal Med., 108 (1995), pp. 62–67

[3] W.J. Taylor Jr., J.R. Vinson; Modeling ballistic impact into flexible materials, AIAA J., 28 (12) (1990), pp. 2098–2103

[4] T.G. Montgomery, P.L. Grady, C. Tomasino; The effects of projectile geometry on the performance of ballistic fabrics, Textile Res. J., 52 (7) (1982), pp. 442–450

[5] H. Kurtaran, M. Buyuk, M. Eskandarian; Ballistic impact simulation of GT model vehicle door using finite element method, Theor. Appl. Fract. Mech., 40 (2) (2003), pp. 113–121

[6] G. Ben-Dor, A. Dubinsky, T. Elperin; Ballistic impact, recent advances in analytical modelling of plate penetration dynamics – a review, Appl. Mech. Rev., Trans. ASME, 58 (2005), pp. 355–371

[7] D.S. Preece, V.S. Berg; Bullet impact on steel and Kevlar steel armor – computer modeling and experimental data, The Proceedings of the ASME Pressure Vessels and Piping Conference – Symposium on Structures Under Extreme Loading (July 2004), pp. 25–29

[8] V.B.C. Tan, T.W. Ching; Computational simulation of fabric armour subjected to ballistic impacts, Int. J. Impact Eng., 32 (11) (2006), pp. 1737–1751

[9] P. Gotts, M. Tawell, S. Holden; Variations in ammunition used for testing personal armour, Personal Armour Systems Symposium (PASS 2010), September 13–17, Quebec, Canada (2010)

[10] R.P. Bixter, C.R. Ahrens, R.P. Rossi, D. Thickman; Bullet identification with radiography, Radiology, 178 (1991), pp. 563–567

[11] G.D. Dodd III, R.F. Budzik Jr.; Identification of retained firearm projectiles on plain radiographs. AJR, 154 (1990), pp. 471–475

[12] M. Mary-Jacque, E.O. Espinoza, M.D. Scanlan; Firearms examinations by scanning electron microscopy: observations and an update on current and future approaches, AFTE J., 24 (3) (1992), pp. 294–303

[13] A. Brandone, G.F. Piancone; Characterisation of firearms and bullets by instrumental neutron activation analysis, Int. J. Appl. Radiat. Isotopes, 35 (5) (1984), pp. 359–364

[14] A.C. Kak, M. Slanley; Principles of Computed Tomography Imaging, IEEE Publishing, New York (1999)

[15] J. Kumar, D. Landheer, J. Barnes-Warden, P. Fenne, A. Attridge, M.A. Williams; Inconsistency in 9 mm bullets measured with non-destructive X-ray computer tomography, Forensic Sci. Int., 214 (2011), pp. 48–58

[16] L.A. Feldkamp, L.C. Davis, J.W. Kress; Practical cone beam algorithm, J. Opt. Soc. Am. (A1 6) (1984), pp. 612–619

[17] J. Kumar, A. Attridge, P.K.C. Wood, M.A. Williams; Analysis of the effect of cone-beam geometry and test object configuration on the measurement accuracy of a computed tomography scanner used for dimensional measurement, Meas. Sci. Technol., 22 (3) (2011) (Article 035105)

[18] W.A. Kalendar; Computed Tomography: Fundamentals, System Technology, Image Quality Applications (3rd ed.), Publicis, Erlangen, Germany (2011)

[19] J. Thornby, D. Landheer, T. Williams, J. Barnes-Warden, P. Fenne, A. Attridge, M.A. Williams; Inconsistency of threat level in soft armour standards, correlation of experimental tests to bullet X-ray 3D images, Personal Armour Systems Symposium (PASS 2012), September 17–21, Nuremberg, Germany (2012)

[20] L. Haag, A. Jason; Where are the bullets? The explanation for the lack of recognizable bullets or significant bullet fragments at certain shooting scenes, AFTE J., 44 (3) (2012), pp. 196–207

[21] B. Planka; Bullet deformation on unyielding targets, AFTE J., 43 (3) (2011), pp. 218–229

[22] R.B. Clough, J.A. Simmons; A theory of multiaxial plasticity based on integral dislocation dynamics, Acta Metall., 22 (5) (1974), pp. 513–521

[23] B. Planka; Evaluation of the terminal strain-hardening border in high-speed impact by means of 3D models, Proceedings of the 10th International Conference on Experimental Mechanics, Lisbon, Portugal (1994)

[24] US Military Standard MIL-STD-662F, V50 Ballistic Test for Armor; US Army Research Laboratory, Weapons & Materials Research Directorate, Aberdeen Proving Ground, MD (December 1997)